A Letters Journal Exploring the Frontiers of Physics

November 2011

EPL, **96** (2011) 40012
doi: 10.1209/0295-5075/96/40012

www.epljournal.org

Readout of a qubit array via a single transmission line

M. Jerger[1], S. Poletto[1], P. Macha[2], U. Hübner[2], A. Lukashenko[1], E. Il'ichev[2] and A. V. Ustinov[1(a)]

[1] *Physikalisches Institut, Karlsruhe Institute of Technology and DFG-Center for Functional Nanostructures (CFN) D-76128 Karlsruhe, Germany, EU*
[2] *Institute of Photonic Technology - PO Box 100239, D-07702 Jena, Germany, EU*

received 25 May 2011; accepted in final form 30 September 2011
published online 10 November 2011

PACS 03.67.Lx – Quantum computation architectures and implementations
PACS 85.25.Am – Superconducting device characterization, design, and modeling

Abstract – Frequency-selective readout for superconducting qubits opens up the way towards scaling qubit circuits without increasing the number of measurement lines. Here we demonstrate the readout of an array of 7 flux qubits located on the same chip using a single measurement line. Each qubit is placed near an individual $\lambda/4$ resonator which, in turn, is coupled to a common microwave transmission line. We performed spectroscopy and coherent manipulation of all qubits and determined their parameters in a single measurement run.

Superconducting qubits are effective two-level quantum systems with a controllable transition frequency between their eigenstates. They are among the most promising candidates for registers of future quantum computers, because of their potential to be manufactured lithographically in a controlled manner. This gives the designer the freedom to construct custom quantum circuits with well-defined parameters and consisting of a large number of devices. In practice, one of the problems that limits the scalability of qubit circuits is the readout apparatus that measures the qubit states at the end of a computation. Traditionally, the quantum state of superconducting flux [1] or phase [2] qubits is read out by measuring the switching current of a SQUID coupled to the qubit. This readout procedure requires dedicated wiring and additional external circuitry for every qubit. An alternative to this bulky readout is a dispersive readout realized by coupling the qubit to a superconducting resonator [3,4]. Using this technique, coupling between 2 and 3 qubits has been investigated [5,6]. A multiplexed readout of two [7] and three [8] qubits through a single resonant cavity has already been demonstrated with transmon qubits. However, this dispersive scheme cannot be scaled to a large number of devices, because one cannot easily distinguish the signals generated by different qubits. A more practical readout system requires discrete channels, each of which communicates the state of a chosen qubit. An approach that is both inherently scalable and provides discrete channels involves frequency-division multiplexing. So far, this method has not been realized for qubit readout, but it was successfully used for kinetic inductance detectors [9] consisting of up to 42 devices [10], and it is easily extendible to measure hundreds of detectors through a single line.

The main message of this letter is reporting a new measurement scheme that is scalable to a large number of superconducting qubits. We present a frequency selective readout of an array of flux qubits that uses a dedicated resonator coupled to each qubit. The basic idea of the measurement is as follows. Due to the coupling to its qubit, each resonator acquires a dispersive shift [4,11],

$$\Delta\omega_{\mathrm{r}} = \pm\frac{\tilde{g}^2}{\omega_{\mathrm{q}} - \omega_{\mathrm{r}}}, \tag{1}$$

depending on the state of the qubit. Here $\tilde{g}$ is the effective coupling between the resonator and the qubit, $\hbar\omega_{\mathrm{q}}$ is the transition energy between the qubit states and $\omega_{\mathrm{r}}/2\pi$ is the resonance frequency of the uncoupled resonator. The positive sign is valid in the ground state of the qubit, and the negative sign in the excited state. Thus, the state of the qubit can be determined by measuring $\Delta\omega_{\mathrm{r}}$. All resonators are coupled to a common transmission line through which their resonance frequencies can be measured.

In this experiment, we used coplanar $\lambda/4$ resonators with resonance frequencies ranging from 9.3 GHz to 10.3 GHz. These resonators were capacitively coupled to a common transmission line on one end and shorted to ground at the other end, see fig. 1. Outside the bands

(a) E-mail: alexey.ustinov@kit.edu

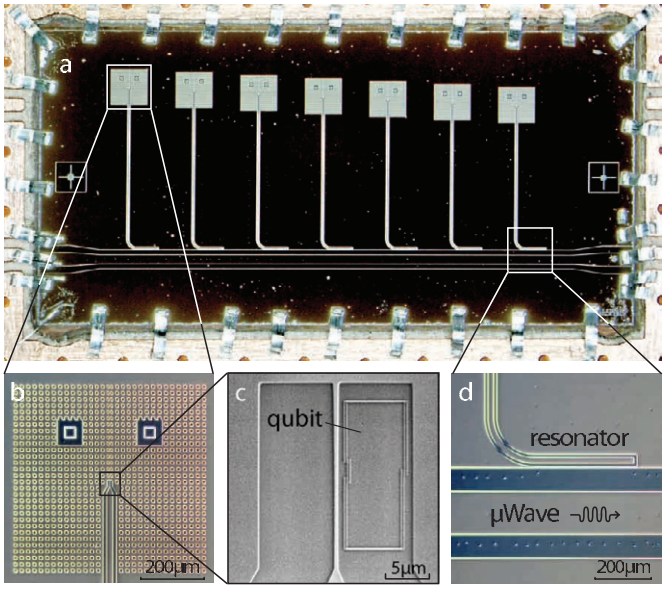

Fig. 1: (Colour on-line) Micrographs of the sample. (a) Overview showing the seven quarter-wave resonators coupled to a common transmission line. (b) Shorted end of one of the resonators. The small holes in the Nb ground plane play the role of magnetic flux traps. (c) One of the flux qubits. (d) An elbow-shaped coupling capacitor between a resonator and the feed line.

of the resonators, electromagnetic waves propagate freely along the feed line. Close to resonance, every resonator acts as a notch filter, which is suppressing transmission through the line by a factor [12]

$$S_{21}(\delta x) = \frac{Q_{\rm L}/Q_0 + 2i\delta x}{1 + 2i\delta x}, \tag{2}$$

where $Q_{\rm L} = (Q_0 Q_{\rm ext})/(Q_0 + Q_{\rm ext})$, Q_0 and $Q_{\rm ext}$ are the loaded, unloaded and external quality factors, respectively, and $\delta x = Q_{\rm L}(\omega - \omega_{\rm r})/\omega_{\rm r}$ is the difference between the resonance and probe frequencies in units of loaded line widths. Close to the minimum, the width of the resonance dip is determined by the internal losses of the resonator, described by the unloaded quality factor Q_0. This feature offers a great advantage over using transmission-type resonators, where the line width is determined by both the losses through the coupling capacitors and the internal loss. With an absorption-type resonator, a small dispersive shift of the resonance frequency, induced by the qubit, results in a large transmission amplitude ratio between the qubit states.

The coupling of the resonators to the feed line must not be too large, to avoid crosstalk between the readout channels. In wireless communications systems, crosstalk is defined as the ratio of interference power to signal power in a channel. For our readout system, this translates into the portion of power absorbed or reflected at the readout frequency by the resonator of an adjacent channel. If multiple reflections on the feed line can be neglected, this ratio is given by $1 - |S_{21}|^2$. In our samples, typical external quality factors $Q_{\rm ext}$ (determined by the coupling capacitors) are about 1500 and unloaded quality factors Q_0 are about 40000 at 30 mK. The frequency spacing of 150 MHz between adjacent channels corresponds to about 20 loaded line widths and results in an expected crosstalk of −32 dB, which is below the noise level of our measurements. The frequency spacing can be reduced to 5 or even 1.5 line widths if a crosstalk of −20 dB or −10 dB is deemed sufficient.

The resonators and the readout line were fabricated by e-beam lithography and CF_4 reactive-ion etching of a 200 nm thick Nb film deposited on an undoped silicon substrate. The aluminium flux qubits were deposited in the gap of each resonator near its shorted end by using the conventional two-angle shadow evaporation technique (fig. 1(b), (c)). They are galvanically decoupled from the resonator, making the qubit fabrication independent of the resonator and providing flexibility in design and fabrication of more complicated circuits. The qubit loop ($7 \times 16\,\mu{\rm m}^2$) is inductively coupled to the resonator, and is interrupted by three Josephson junctions. Two of them have a nominal size of $700 \times 200\,{\rm nm}^2$, while the third junction, called α-junction, is about 30% smaller. The transition frequency between the ground and first-excited states of a flux qubit is given by [13]

$$\omega_{\rm q} = \sqrt{\Delta^2 + \epsilon^2}. \tag{3}$$

Here $\Delta/2\pi$ is the minimum transition frequency between the ground and first-excited states, at the symmetry point of the flux qubit. The energy bias $\epsilon = 2I_{\rm p}(\Phi - \Phi_0/2)/\hbar$, expressed here in frequency units, is caused by the external magnetic flux Φ applied to the qubit loop. Thus, the transition frequency can be controlled by changing the external magnetic field applied to the qubit.

In order to demonstrate that our probe signal reads out the quantum states of the qubits, we carried out spectroscopic measurements. Two microwave signals are applied to the feed line: one excites the qubit and thereby changes the dispersive shift of the resonator frequency due to the qubit state. Another one weakly probes the resonator frequency. Because we designed relatively low external quality factors $Q_{\rm ext}$ of the resonators, corresponding to a large coupling capacitor between the transmission line and resonators, we can apply the excitation tone directly to the line that feeds the resonators and do not need any additional line to manipulate the qubits. In devices #1–#6, the observed frequency shift is several (unloaded) line widths, yielding a difference in transmission between the two qubit states of well above 10 dB. Device #7 has a lower Q_0 of 5000, yielding a difference of less than 3 dB. Using the technique described above, we measured the spectra of all seven qubits. The probe signal was kept sufficiently small to achieve an average photon number in the resonators below unity. This condition was verified by ac Zeeman shift measurements (not shown). The spectra, shown in fig. 2,

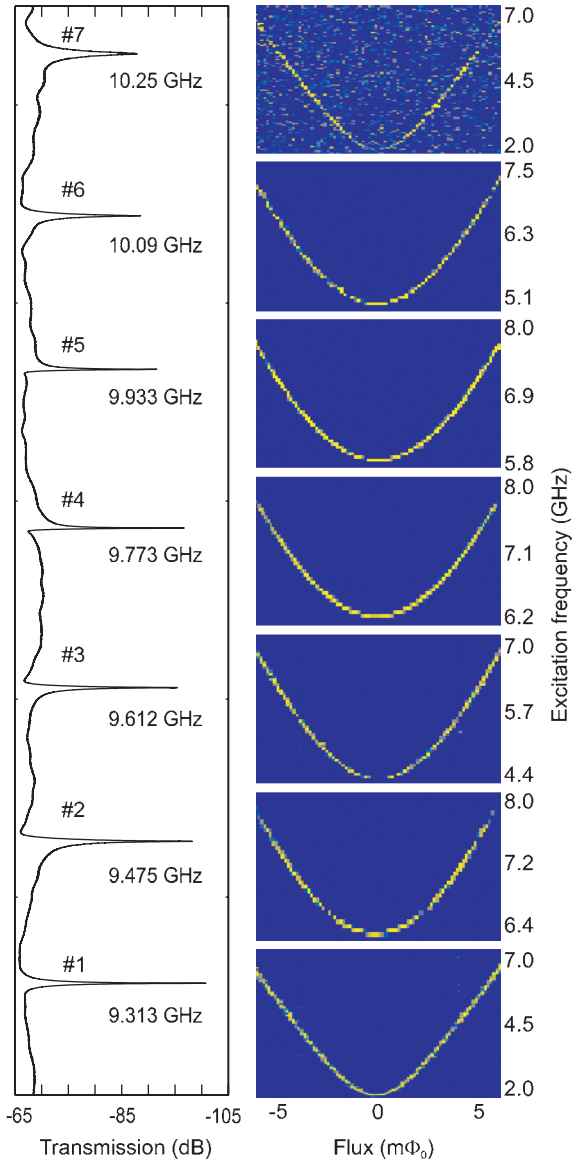

Fig. 2: (Colour on-line) Left: transmission spectrum of the sample, showing absorption dips of the seven resonators at zero flux bias. Right: spectroscopy of the corresponding seven flux qubits close to their respective symmetry points. Flux scales are shown relative to the symmetry points of the qubits. Each spectrum is shown next to the transmission dip of the corresponding readout resonator.

contain important fabrication parameters of the qubits. We combine spectroscopy data with the dispersive shift at a chosen bias point and make use of eq. (1) to extract the bare coupling g between each resonator and qubit. Interactions between a qubit and the readout resonator of a different qubit were not observed, as expected due to the above-mentioned very small crosstalk between the channels. A qubit-qubit coupling could be implemented using an additional dedicated bus resonator [7] that couples to all qubits. The persistent current I_p circulating in the qubit loop is obtained from a fit of the transition frequency

Table 1: Qubit gaps Δ, bare coupling strengths g, persistent currents I_p, T_1 and T_2 times extracted from measurements.

Qubit	$\Delta/2\pi$ (GHz)	$g/2\pi$ (MHz)	I_p (nA)	T_1 (ns)	T_2 (ns)
1	1.97	51	159		
2	6.35	73	120	1100	180
3	4.40	80	134	990	145
4	6.17	85	126	970	120
5	5.80	89	129	900	70
6	5.10	89	132	650	200
7	2.00	51	163		

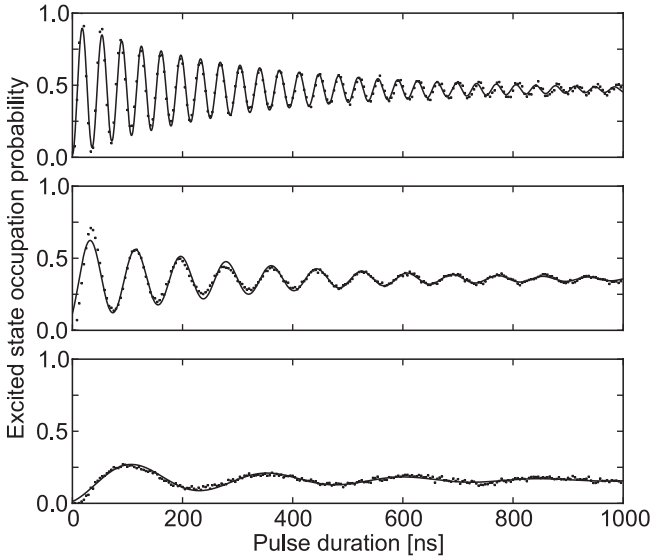

Fig. 3: Rabi oscillations of qubit #2 at $-75\,\mathrm{dBm}$ (top), $-82.5\,\mathrm{dBm}$ (middle) and $-92.2\,\mathrm{dBm}$ (bottom) of excitation power into the feed line. The Rabi frequencies $\omega_\mathrm{Rabi}/2\pi$ are 28 MHz, 12.3 MHz and 4 MHz, respectively, satisfying $f_\mathrm{Rabi} \propto \sqrt{P_\mathrm{exc}}$. All curves were fitted with $T_1 = 1100\,\mathrm{ns}$ and $T_2 = 180\,\mathrm{ns}$. A fit to the steady-state occupation probability at different excitation powers was used to calibrate the readout.

vs. flux bias curve using eq. (3). The measured qubit parameters are summarized in table 1. Note that all spectra were measured in a single run.

To characterize the coherent properties of the qubits, we applied pulsed excitation and probe signals. After an excitation pulse of variable duration and amplitude, a 500 ns probe tone was sent through the measurement line. The transmitted probe pulse was down-converted using an IQ-mixer, acquired by a transient recorder and processed digitally. This rather long probe pulse was chosen to maximize the amount of qubit state information acquired per trace. Rabi oscillations of the qubit were observed when varying the duration of the excitation pulse, shown in fig. 3. Fits to these oscillations at different excitation powers confirm that the oscillation frequency is proportional to the excitation amplitude, as expected [14].

Energy relaxation (T_1) times were measured by varying the time delay between the excitation and probe pulses. Dephasing (T_2) times were extracted from the decay of Rabi oscillations, using the relation [14] $2/T_{\mathrm{Rabi}} = 1/T_1 + 1/T_2$. The dynamical qubit parameters are summarized in table 1.

Table 1 shows that the reproducibility of the qubit parameters is rather good. For the qubits in the middle of the chip (#2–#6) the spread of the persistent current values is below 5%. The spread of the qubit gap is higher (above 20% —due to its exponential dependence on the critical current of the α-junction). Remarkable is also the relatively strong coupling g (see table 1), which is due to purely inductive interaction. The T_1 times of 900 ns with a spread of 20% and T_2 times of 150 ns with a spread of 35% are reasonable for flux qubits. The deviations of the parameters of qubits #1 and #7 (especially coupling which differs by almost 50% compared to the others) are currently under investigation.

In conclusion, we have demonstrated a frequency multiplexing readout for superconducting qubits, which makes it possible to perform spectroscopy as well as coherent manipulation of many qubits using a single on-chip transmission line. The reported readout scheme is not limited to flux qubits and can easily be implemented for other types of superconducting qubits. It overcomes the scalability limitations of the conventional readout of superconducting qubit circuits and opens the possibility of building up quantum registers with hundreds of qubits.

* * *

This work was supported by the EU project SOLID, the Deutsche Forschungsgemeinschaft (DFG), and the State of Baden-Württemberg through the DFG-Center for Functional Nanostructures (CFN) within sub-project B3.4.

REFERENCES

[1] van der Wal C. H. *et al.*, *Science*, **290** (2000) 773.
[2] Martinis J. M., Nam S., Aumentado J. and Urbina C., *Phys. Rev. Lett.*, **89** (2002) 117901.
[3] Il'ichev E. *et al.*, *Phys. Rev. Lett.*, **91** (2003) 097906.
[4] Wallraff A. *et al.*, *Nature*, **431** (2004) 162.
[5] Grajcar M. *et al.*, *Phys. Rev. B*, **72** (2005) R020503.
[6] Izmalkov A. *et al.*, *Europhys. Lett.*, **76** (2006) 533.
[7] Majer J. *et al.*, *Nature*, **449** (2007) 443.
[8] DiCarlo L. *et al.*, *Nature*, **467** (2010) 574.
[9] Day P. K., Leduc H. G., Mazin B. A., Vayonakis A. and Zmuidzinas J., *Nature*, **425** (2003) 817.
[10] Monfardini A. *et al.*, *Astron. Astrophys.*, **521** (2010) A29.
[11] Blais A., Huang R.-S., Wallraff A., Girvin S. M. and Schoelkopf R. J., *Phys. Rev. B*, **69** (2004) 062320.
[12] Mazin B. A., *Microwave Kinetic Inductance Detectors*, PhD Thesis, California Institute of Technology, 2004.
[13] Mooij J. E. *et al.*, *Science*, **285** (1999) 1036.
[14] Abragam A., *The Principles of Nuclear Magnetism* (Oxford University Press, Glasgow) 1961.